doi: 10.4149/gpb_2023009

Weighted gene coexpression network analysis reveals negative regulation of hypertrophic cardiomyopathy by carboxylesterase 1 and cathepsin C

Ye Kuang, Jia Wang, Yulin Dong, Yun Cheng, Hongyan Li, Yong Ji, Hui Gao and Xianghong Cao

Department of Medical Laboratory, Yan'An Hospital of Kunming city, Kunming, China

Abstract. Hypertrophic cardiomyopathy (HCM) is a primary cardiomyopathy characterized by hypertrophic cardiomyocytes. It is one of the leading causes of sudden death in adolescents. However, the molecular mechanism of HCM is not clear. In our study, ribonucleic acid (RNA) sequence data of myocardial tissue in HCM patients were extracted from the Gene Expression Omnibus (GEO) database (GSE130036) and analyzed by weighted gene coexpression network analysis (WGCNA). A total of 31 coexpression modules were identified. The coexpression black module significantly correlated with maximum left ventricular wall thickness (Maxi LVWT). We screened the differentially expressed mRNAs between normal tissues and HCM tissues using the dplyr and tidyr packages in R3.6.2. The genes in the black module and differentially expressed genes were further intersected. We found that the expression of carboxylesterase 1 (CES1) and cathepsin C (CTSC) was downregulated in HCM tissues and negatively correlated with Maxi LVWT. We further verified the expression of CES1 and CTSC was downregulated in HCM clinical blood and negatively correlated with Maxi LVWT. Finally, we demonstrated that overexpression of CTSC and CES1 could alleviate HCM in an HCM cell model. In summary, the study suggests that CES1 and CTSC negatively regulate the development of HCM and have potential as therapeutic and diagnostic targets for HCM.

Key words: WGCNA — Carboxylesterase 1 — Cathepsin C — Hypertrophic cardiomyopathy — Maximum left ventricular wall thickness

Abbreviations: Ang II, angiotensin II; ANP, atrial natriuretic peptide; β-MHC, major histocompatibility complex beta; BNP, brain natriuretic peptide; CES1, carboxylesterase 1; CTSC, cathepsin C; DEmRNAs, differentially expressed mRNAs; FC, fold change; GEO, Gene Expression Omnibus; HCM, hypertrophic cardiomyopathy; LAD, left atrial diameter; LVST, left ventricular septal thickness; LVEDD, left ventricular end-diastolic; LVEF, left ventricular ejection fraction; Maxi LVOTG, maximum left ventricular outflow track gradient at rest or after exercise; Maxi LVWT, maximum left ventricular wall thickness; PCC, Pearson's correlation coefficient; PSN, penicillin-streptomycin-neomycin; SPSS, statistical product and service solutions; WGCNA, weighted gene coexpression network analysis.

Electronic supplementary material. The online version of this article (doi: 10.4149/gpb_2023009 contains Supplementary material.
Correspondence to: Hui Gao, Yan'An Hospital of Kunming city, 245 People East Road, Kunming 650000, Yunnan Province, China
E-mail: gaohui19@yeah.net
Xianghong Cao, Yan'An Hospital of Kunming city, 245 People East Road, Kunming 650000, Yunnan Province, China
E-mail: guotiao@sina.com

Introduction

Hypertrophic cardiomyopathy (HCM) is a kind of primary cardiomyopathy characterized by hypertrophy of cardiomyocytes. HCM has clear genetic characteristics, which is chromosome dominant inheritance (Maron 2012). The clinical manifestations of HCM are asymmetrical ventricular wall hypertrophy, smaller ventricular cavity, increased or constant ejection fraction, left ventricular outflow tract obstruction, diastolic dysfunction, myocardial ischemia and other symptoms (Marian and Braunwald 2013; Canepa et al. 2016; Lu et al. 2018). However, the clinical symptoms of HCM are not obvious, and the patients are difficult to identify. Severe patients may have heart failure or even sudden death (Efthimiadis et al. 2014; Liew et al. 2017). At present, HCM has become one of the main causes of sudden adolescent death.

The pathogenesis of HCM reflects the mutation and diversity of pathogenic genes. The occurrence and development of HCM are divided into four interlocking mechanisms: (1) Familial chromosome mutation. At present, it has been confirmed that at least 14 gene mutations are related to the pathogenesis of HCM (Wang et al. 2013), and 10 of them are genes encoding sarcomere structural proteins (Marques and de 2016). (2) Mutated genes directly lead to abnormal structure and function of coding proteins, such as sarcomere cell protein, which is the key protein of pathogenesis (Kamisago et al. 2000). (3) Gene regulation is a complex network regulation process. Changes in gene expression levels will lead to the activation or closure of HCM-related signaling pathways, such as the MAPK (Josowitz et al. 2016) and TGF-β1 signaling pathways (Vakrou et al. 2018). (4) Changes in these molecules and pathways lead to the occurrence of HCM. Therefore, HCM is the result of the interaction of pathogenic genes, mutated genes and abnormal signaling pathways. Some studies have investigated the abnormal expression of mRNA, microRNA (miRNA) and long noncoding RNA (lncRNA) in the pathogenesis of HCM and characterized their roles in HCM pathogenesis. For example, Wei Yang and colleagues found that 1426 lncRNAs and 1715 mRNAs were aberrantly expressed in HCM patients and that lncRNA–mRNA coexpression systems were mostly enriched in ribosomes and oxidative phosphorylation (Yang et al. 2015). Some studies constructed lncRNA–miRNA-mRNA regulatory networks based on differentially expressed RNAs. For example, Jiajianghui Li and colleagues integrated four expression profiles (GSE36961, GSE36946, GSE68316 and GSE32453) and constructed lncRNA–miRNA-mRNA and protein–protein networks that regulated the process of HCM (Li et al. 2019).

In our study, ribonucleic acid (RNA) sequence data of myocardial tissue in HCM patients were extracted from the Gene Expression Omnibus (GEO, https://www.ncbi.nlm.nih.gov/geo/query/acc.cgi?acc = GSE130036) database (GSE130036) and analyzed by weighted gene coexpression network analysis (WGCNA). We found that the expression level of carboxylesterase 1 (CES1) and cathepsin C (CTSC) was downregulated in HCM tissues and negatively correlated with maximum left ventricular wall thickness (Maxi LVWT). We further verified this conclusion in clinical samples from HCM patient blood. Finally, we demonstrated that overexpression of CTSC and CES1 could alleviate HCM in an HCM cell model. Carboxylesterase is a kind of esterase that is widely expressed in bacteria and humans. According to the homology of the amino acid sequence, carboxylesterases can be divided into five categories: CES1–CES5. CES1 is involved in the hydrolysis of exogenous and endogenous compounds containing ester groups, including several basic and commonly used drugs, such as clopidogrel, temocapril and imidapril (Rasmussen et al. 2015). CTSC, also known as dipeptidyl peptidase I, is a lysosomal cysteine protease that is essential for the catalytic activation of many serine proteases (Shen et al. 2021). CTSC can activate serine protease in hematopoietic cells and has relatively high expression in inflammatory cells such as neutrophils, natural killer cells, cytotoxic T cells, mast cells and alveolar macrophages (Pham et al. 1997). CTSC is involved in many biological processes, such as the regulation of glycosidase activity, and the activation of inflammatory- and immune-related granzymes (Minarowska et al. 2012; Shen et al. 2021). However, the role of CES1 and CTSC in hypertrophic cardiomyopathy has not been reported. In our study, we suggest that CES1 and CTSC negatively regulate the development of HCM and have potential as therapeutic and diagnostic targets for HCM.

Materials and Methods

Data collection

The RNA expression data (high throughput sequencing) of myocardial tissues from 28 HCM patients and 9 healthy donors were downloaded from the GEO database. The RNA expression matrix was pretreated to remove the genes with more than 20% missing value (value = 0). Clinical and demographic data of 28 HCM patients were obtained from the citation of Liu et al. (2019), including sex, age, smoking, LAD (left atrial diameter), LVST (left ventricular septal thickness), LVEDD (left ventricular end-diastolic), LVEF (left ventricular ejection fraction), Maxi LVWT, Maxi LVOTG (maximum left ventricular outflow track gradient at rest or after exercise) and sample location. The GSE68316 dataset was a microarray profiling of lncRNAs and mRNAs associated with HCM. Myocardial tissues were obtained from 7 HCM patients and 5 disease-free individuals, and lncRNA and mRNA expression profiles were analyzed using CapitalBio Human LncRNA Microarray v2.0.

Clinical sample collection

Forty peripheral blood samples were obtained from HCM patients (n = 20) or healthy people (n = 20) between November 2020 and May 2021 in the Kunming Yan'an Hospital (Kunming, China). This study was approved by the Ethics Committee of the Kunming Yan'an Hospital (Kunming, China; approval No. 2019-058-01), and all patients signed consent forms. We collected clinical information for all patients. The clinical features of the patients, including sex, age, LAD, LVST, LVEDD, LVEF, Maxi LVWT and sample location were collected from their medical records.

Cell culture and treatment

The human cardiomyocyte cell line (AC16) was purchased from Cobioer Biosciences Co., Ltd. AC16 cells were cultured in Dulbecco's modified Eagle medium (cat. no. 11965092; Thermo Fisher Scientific, Inc.) containing 10% fetal bovine serum (cat. no. 16140089; Thermo Fisher Scientific, Inc.) and 1% penicillin streptomycin neomycin (PSN) antibiotic mixture (cat. no. 15640055; Thermo Fisher Scientific, Inc.). Cells were grown with 5% CO_2 at 37°C. pCMV3-C-GFPSpark (cat. no. CV026; Sino Biological, Inc.) was used as an overexpression vector to construct the pCMV3-CES1 or pCMV3-CTSC recombinant plasmid. pCMV3-untagged (cat. no. CV011; Sino Biological, Inc.) was used as the negative control. The plasmids (20 pmol) were added to 50 μl opti-MEM (cat. no. 11058021; Thermo Fisher Scientific, Inc.) medium without serum. Lipofectamine™3000 (1 μl, cat. no. L3000008; Thermo Fisher Scientific, Inc.) was also added to 50 μl opti-MEM serum-free medium. The mixture was added to the cell suspension, which was cultured at 37°C and 5% CO_2. After 48 h, other experimental steps were carried out. AC16 cells were treated with 150 nM Ang II (cat. no. A9290; Beijing Solarbio Science&Technology Co., Ltd) for 24 h, which was used to model hypertrophic cardiomyopathy.

Quantitative reverse transcription PCR

Total RNA was extracted from the peripheral blood using a GenElute™ plasma/serum RNA purification midi kit (Product Number: RNB600; Sigma-Aldrich LLC.) according to the manufacturer's instructions. The concentration of total RNA was detected by a NanoDrop One spectrophotometer (art.no. ND-ONE-W; Thermo Fisher Scientific, Inc.). Total RNA was reverse transcribed into cDNA, and quantitative real-time PCR (qPCR) was performed using the TaqMan One Step RT-qPCR Kit (cat. no. T2210; Beijing Solarbio Science&Technology Co., Ltd) in a real-time fluorescent quantitative PCR instrument (model: ABI7500; Thermo Fisher Scientific, Inc.). The following primer sequences were used for qPCR: CES1 forward, 5'- CTGTGTAACGCTCCTCCTGTG-3' and reverse, 5'-CCCAGCACAGGGATCACATC-3'; CTSC forward, 5'-CACAGATGGCCCTCTCAAGG-3' and reverse, 5'-CAGGGGCTGATACCAAGGAC-3'; GAPDH forward, 5'-ATGACATCAAGAAGGTGGTGAAGCAGG-3' and reverse, 5'-GCGTCAAAGGTGGAGGAGTGGGT-3'; ANP (Atrial natriuretic peptide) forward, 5'-CACAGCATCAGAAAGCCCCC-3' and reverse, 5'-AGTGGATTGCTCCTTGACGA-3'; BNP (Brain Natriuretic Peptide) forward,5'-GCTGCTCCTGCAATGAATGG-3' and reverse, 5'-TGGAAACGTCCGGGTTACAG-3'; β-MHC (major histocompatibility complex beta) forward, 5'-AAGCTTTTTCCGCTGCACTG-3' and reverse, 5'-GGAAGGTAAGTCCCGCTCAC-3'. The difference in mRNA expression between the normal and HCM groups was calculated using the $2^{-\Delta\Delta Cq}$ method (Schmittgen and Livak 2008). GAPDH was used as an internal reference for standardization.

Weighted correlation network analysis (WGCNA) of mRNAs

WGCNA aims to find coexpressed gene modules and explore the relationship between the gene network and concerned phenotypes (Langfelder and Horvath 2008). The RNA expression matrix was preprocessed to remove the genes with more than 20% missing values (value = 0) and the rest were $\log_{10}^{(TPM + 0.001)}$ standardized from the GSE130036 dataset. We then screened the protein-coding genes from processed RNA expression data using the dplyr and tidyr packages in R3.6.2 software (https://www.r-project.org/), according to *Homo sapiens GRCh38.94*. A total of 14348 genes were included in the WGCNA. First, a sample tree was established, and the outlier samples were removed. A sample dendrogram and heatmap of clinical traits were visualized by the WGCNA package. A soft-thresholding power (β) was selected to establish an adjacent matrix according to the degree of connectivity so that our gene distribution fit into the scale-free network. The proximity matrix and topological matrix were obtained according to the β value, and the memory network was verified to be close to scale free under the selected β value. The genes were clustered, and then the tree was cut into different color modules using the dynamic tree cut method. Four hundred genes were randomly selected to draw a topological overlapping heatmap. Pearson's correlation coefficient (PCC) between module eigengenes and clinical traits was analyzed. According to the correlation and p value, the modules related to specific clinical traits were explored. The mRNAs involved in the key modules were considered to be highly interconnected with the specific clinical traits.

Screening for differentially expressed mRNAs (DEmRNAs)

DEmRNAs between normal samples and HCM samples in the GSE130036 or GSE68316 dataset were screened by us-

ing the limma package in R3.6.2 software. Adjusted p values <0.05 and $|\log^{\text{fold change (FC)}}| > 1.5$ were set as the strict thresholds. The visualization of DEmRNAs was performed using Volcano map and pheatmap packages in R3.6.2.

Enzyme-linked immunosorbent assay (ELISA)

ELISA was used to detect the contents of CES1, CTSC, ANP, BNP and β-MHC in peripheral blood or cell lines according to the manufacturer's instructions (cat. nos. EH64RBX5, EH73RB, EIAANP, and EHNPPB; Thermo Fisher Scientific, Inc; cat. no. kt98804, Wuhan Mosak Biotechnology Co., Ltd). The optical density of all the ELISA kits was determined at OD450 nm using a microplate photometer (model: Multiskan FC; Thermo Fisher Scientific, Inc.).

Statistical analysis

Statistical analysis of all data was performed using the R programming language (Version 3.6.2) and statistical product and service solutions (SPSS) 15.0 software. All experiments were repeated at least five times for statistical calculation and the data were expressed as means ± standard deviations (SD). A two-tailed unpaired Student's t test was used to determine the statistical significance of the experimental results. One-way ANOVA with the least significant difference *post hoc* test was used for the comparison of multiple groups. The Pearson correlation coefficient was used to calculate the correlation between relative gene expression and Maxi LVWT. $p < 0.05$ showed statistical significance.

Results

Construction of coexpression modules of HCM

A total of 14,348 mRNAs from the GSE130036 dataset were included in the WGCNA. According to the mRNA expression matrix, we clustered the samples and eliminated the outliers. Among the 28 HCM samples, there was no obvious outlier, which could be used for subsequent WGCNA (Fig. 1A). We collected clinical data of 28 HCM patients included sex, age, smoking, LAD, LVST, LVEDD, LVEF, Maxi LVWT, Maxi LVOTG and sample location (Table 1). Based on mRNA

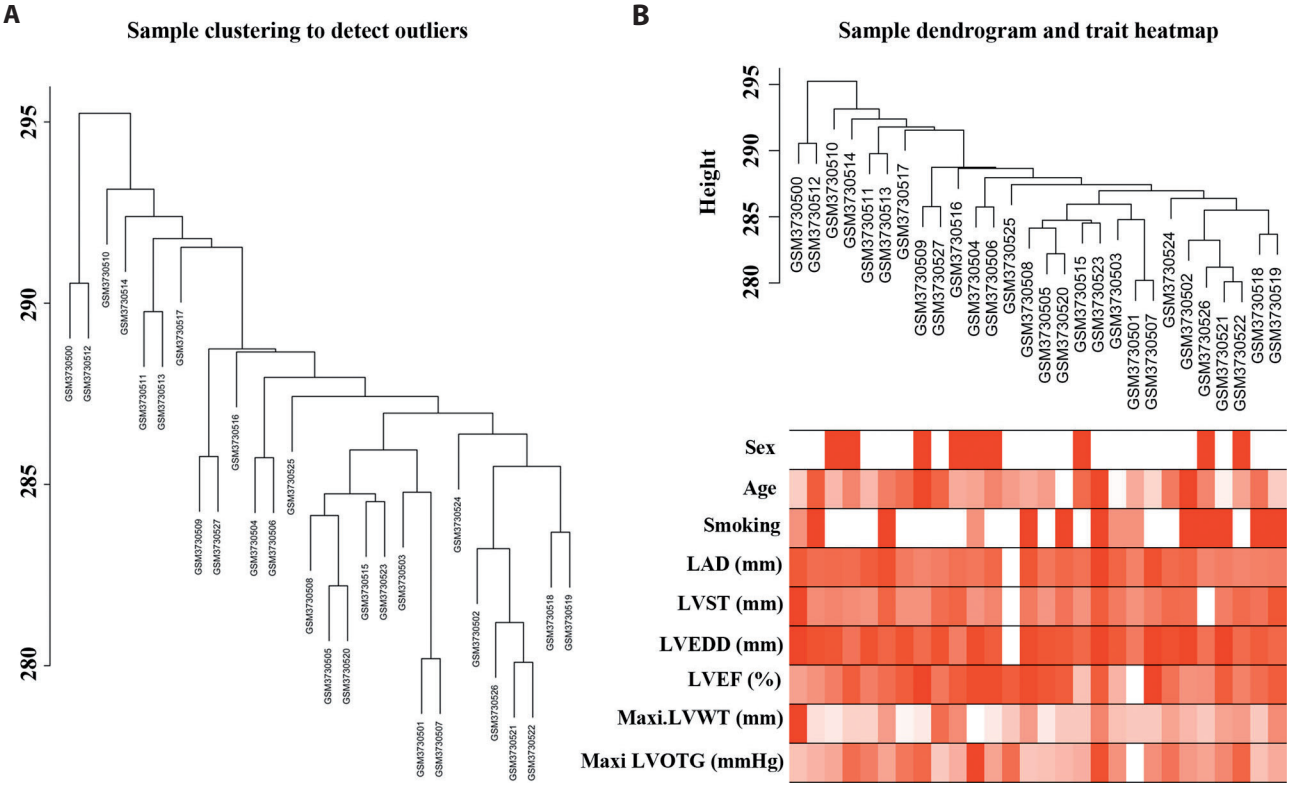

Figure 1. Sample cluster analysis based on the RNA expression matrix from the GEO database (GSE130036). **A.** Sample cluster based on RNA expression data. **B.** The sample dendrogram and trait heatmap based on mRNA expression data and clinical data. GEO, gene expression omnibus; LAD, left atrial diameter; LVST, left ventricular septal thickness; LVEDD, left ventricular end-diastolic; LVEF, left ventricular ejection fraction; Maxi LVWT, maximum left ventricular wall thickness; Maxi LVOTG, maximum left ventricular outflow track gradient at rest or after exercise; GSM, GEO sample.

expression data and clinical data, we grouped the sample dendrogram and trait heatmap (Fig. 1B). According to the power value (β = 6) and scale R^2 value, the independence and the average connectivity of the coexpression module were defined (Fig. 2A). We checked whether the memory network approximated scale free under the selected β value. As shown in Figure 2B, κ was negatively correlated with p(κ) ($R^2 = 0.86$), indicating that the selected β value (β = 6) could establish a scale-free gene network. Therefore, we defined the adjacency matrix with β = 6 and constructed the coexpression gene module. There were 31 coexpression modules of coexpressed genes in WGCNA (Fig. 2C). The number of genes in the corresponding module was shown in Table 2. The gene network was visualized using a heatmap that depicted the topological overlap matrix (TOM) among the top 400 genes in the analysis (Fig. 2D).

Table 1. Clinical features of HCM tissue samples from GSE130036 data set

Clinical characteristics		
Age (year)	Media	32
	Mean	33.4
	Range	24–54
Sex (*n*)	Female	9
	Male	19
Smoking (*n*)	Yes	10
	No	4
	Unknown	14
LAD (mm)	Media	41
	Mean	42.6
	Range	36–62
LVST (mm)	Media	20
	Mean	20.8
	Range	12–29
LVEDD (mm)	Media	46
	Mean	45.7
	Range	35–51
LVEF (%)	Media	69.5
	Mean	70.4
	Range	50–80
Maxi LVWT (mm)	Media	26
	Mean	25.2
	Range	16–38
Maxi LVOTG (mmHg)	Media	75.7
	Mean	70
	Range	30–126
Sample location	Left ventricular septum	28

LAD, left atrial diameter; LVST, left ventricular septal thickness; LVEDD, left ventricular end-diastolic; LVEF, left ventricular ejection fraction; Maxi LVWT, maximum left ventricular wall thickness; Maxi LVOTG, maximum left ventricular outflow track gradient at rest or after exercise.

Table 2. Number of genes in 31 co-expression modules

Module color	Number of genes
black	578
blue	743
cyan	505
steelblue	75
lightgreen	479
red	580
magenta	553
white	446
purple	553
tan	529
salmon	527
darkgrey	462
darkturquoise	463
brown	715
lightyellow	479
grey	3008
turquoise	1676
darkgreen	485
green	593
pink	564
yellow	691
darkorange	448
lightcyan	494
greenyellow	549
orange	456
grey60	485
skyblue	398
midnightblue	505
saddlebrown	377
darkred	468
royalblue	471

Coexpression modules related to clinical traits

The GSE130036 dataset provides the following clinical data, including sex, age, smoking, LAD, LVST, LVEDD, LVEF, Maxi LVWT, Maxi LVOTG and sample location. We drew a heatmap of the correlation between the gene coexpression module and clinical traits. As shown in Figure 3, the coexpression black module was significantly associated with Maxi LVWT (R = 0.61, $p = 5\times10^{-4}$). We further plotted the scatter plot of gene significance for Maxi LVWT and module membership in the black module. The high correlation can be revealed that gene significance for Maxi LVWT was highly associated with module membership in the black module (cor = 0.74, $p = 2.8\times10^{-101}$; Fig. 4C). Therefore, we chose the genes in the black module for further analysis.

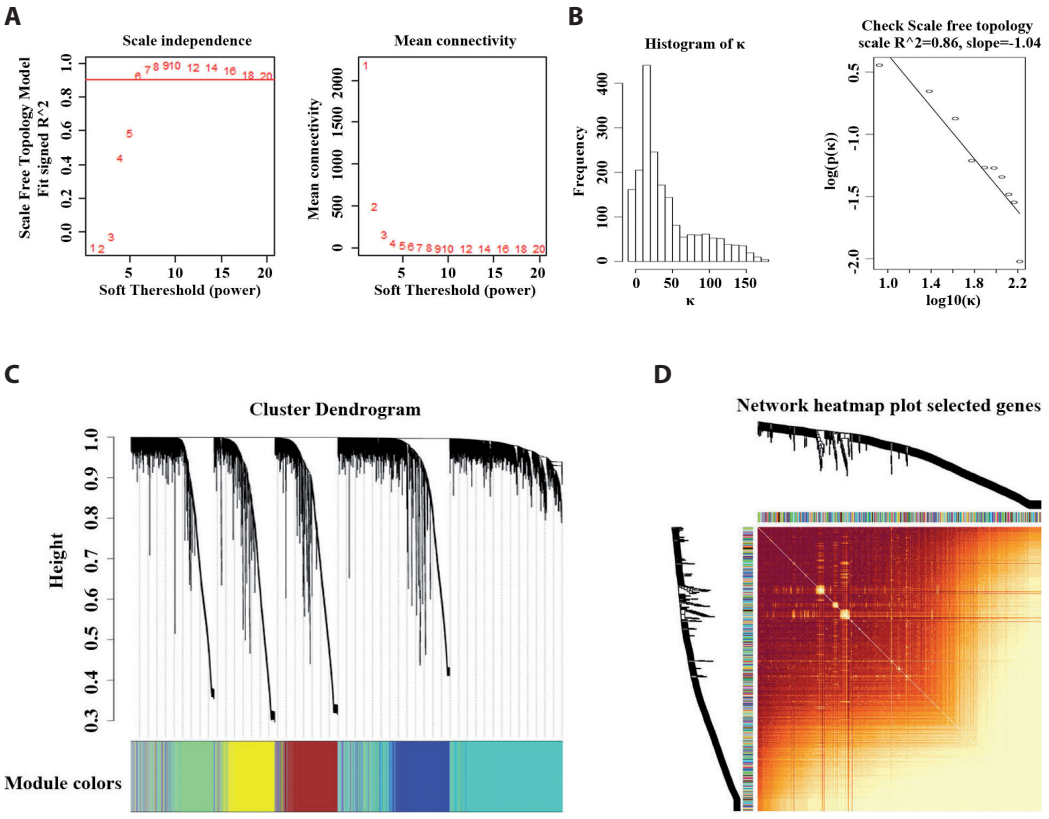

Figure 2. Construction of coexpression modules in HCM. **A.** The various soft-threshold powers were analyzed based on network topology. Select the best soft threshold with $\beta = 6$. The x-axis shows the soft-threshold powers. The y-axis on the left shows the correlation between connectivity κ and p (κ). The y-axis on the right shows the mean connectivity. **B.** Verification of the constructed scale-free network. $R^2 = 0.86$; slope = −1.04. **C.** Clustering dendrogram of mRNAs and original modules. There were 31 coexpression modules of coexpressed genes in the WGCNA. **D.** The gene network was visualized using a heatmap plot that depicted the topological overlap matrix (TOM) among the top 400 mRNAs in the analysis. HCM, hypertrophic cardiomyopathy; WGCNA, weighted gene coexpression network analysis.

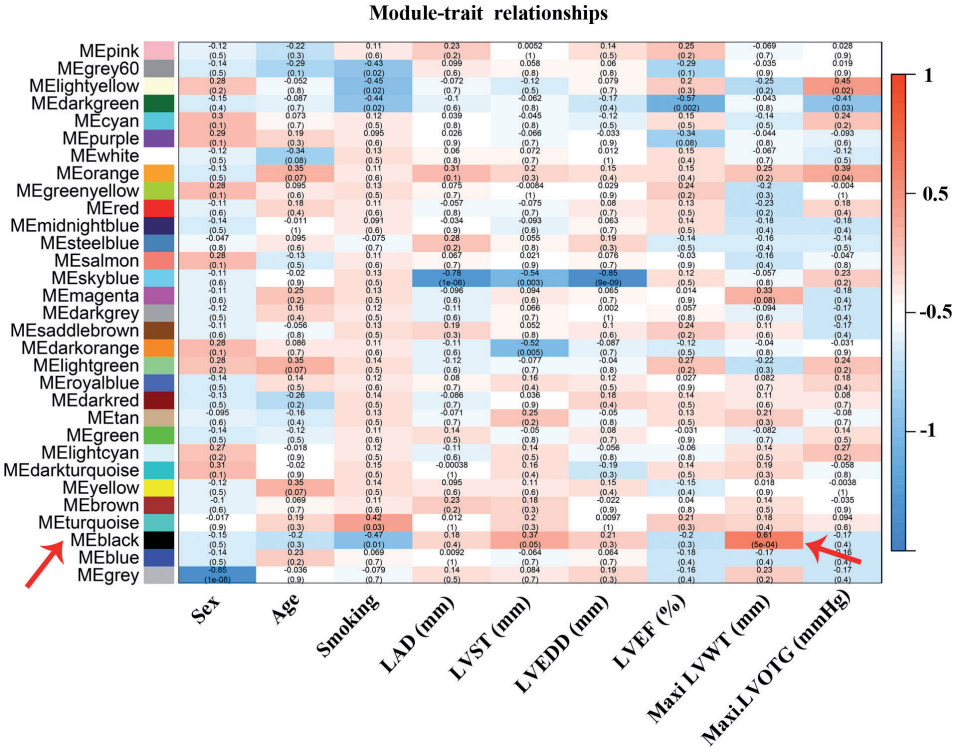

Figure 3. Coexpression modules related to clinical traits. Each row represents the different coexpression modules. Each column represents the different clinical traits. Each cell contains the corresponding correlation value and p value. The red arrow represented the selected black module and its association with Maxi LVWT. For abbreviations, see Figure 1.

The core genes were further screened by differential expression analysis

A total of 132 mRNAs were differentially expressed between HCM samples and normal samples (adjusted p value < 0.05 and $|\log^{FC}| > 1.5$). Compared with the expression of mRNAs in HCM samples, 41 mRNAs (31.06%) were upregulated in the normal samples, while the 91 mRNAs (68.94%) were downregulated in the normal samples (Supplementary Material, Table S1). The differences in the expression of mRNAs between the normal samples and HCM samples were subjected to hierarchical clustering analysis and visualized by

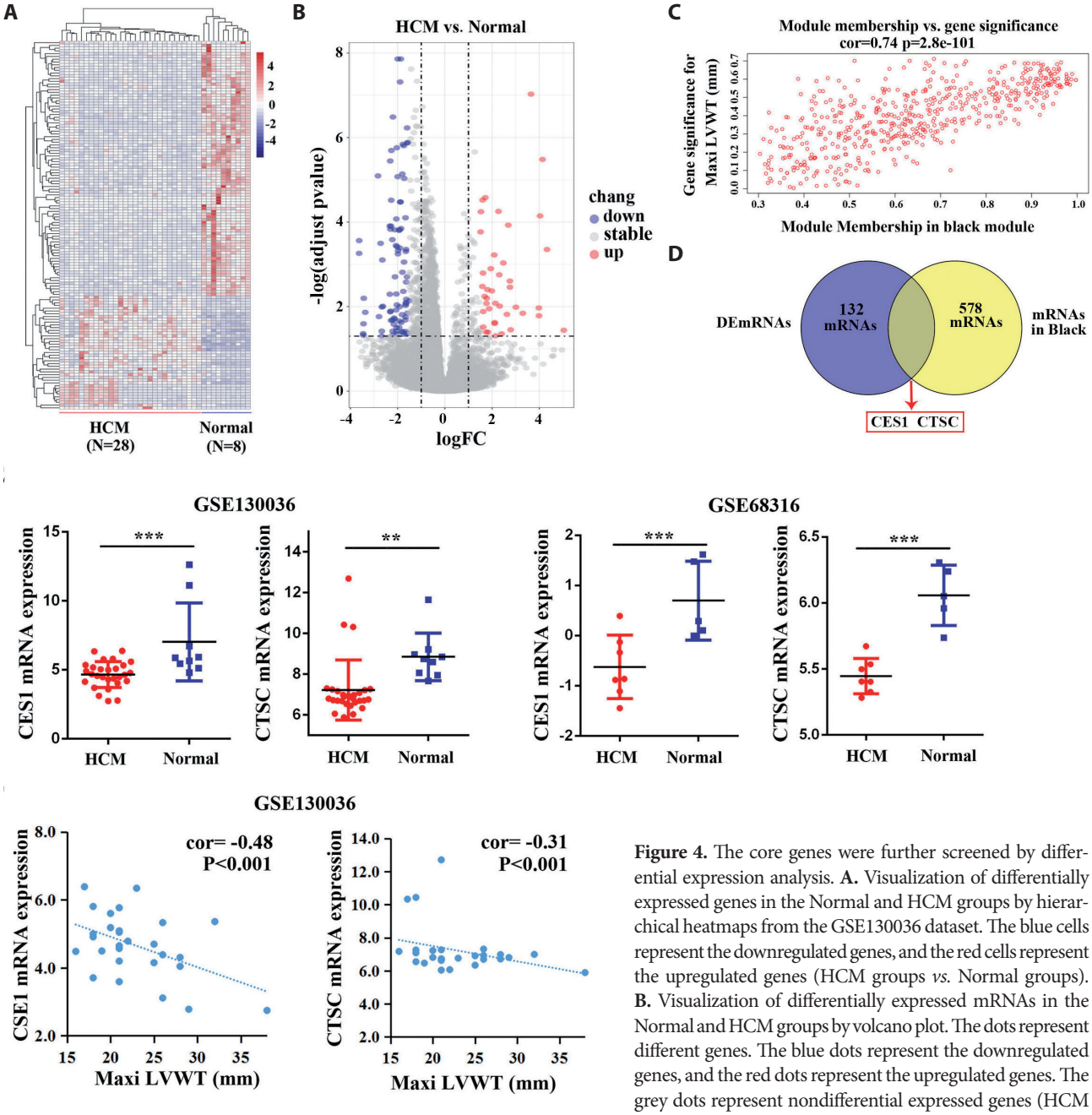

Figure 4. The core genes were further screened by differential expression analysis. **A.** Visualization of differentially expressed genes in the Normal and HCM groups by hierarchical heatmaps from the GSE130036 dataset. The blue cells represent the downregulated genes, and the red cells represent the upregulated genes (HCM groups *vs.* Normal groups). **B.** Visualization of differentially expressed mRNAs in the Normal and HCM groups by volcano plot. The dots represent different genes. The blue dots represent the downregulated genes, and the red dots represent the upregulated genes. The grey dots represent nondifferential expressed genes (HCM groups *vs.* Normal groups). **C.** Scatterplot of gene significance for Maxi LVWT *vs.* module membership in the black module. **D.** CES1 and CTSC were obtained from the intersection of genes with different expression and genes in the black module. **E.** The scatter plot shows the mRNA expression of CES1 and CTSC in the HCM and Normal groups according to GSE130036 or GSE68316 data. *** $p < 0.001$, ** $p < 0.01$ *vs.* HCM group. **F.** mRNA expression of CES1 or CTSC was negatively correlated with Maxi LVWT in GEO130036 data. HCM, hypertrophic cardiomyopathy; GEO, gene expression omnibus; CES1, carboxylesterase 1; CTSC, cathepsin C; Maxi LVWT, maximum left ventricular wall thickness.

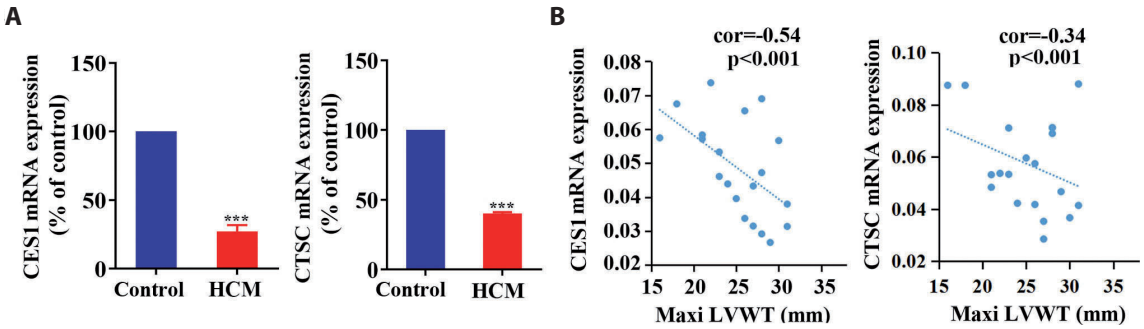

Figure 5. Clinical sample validation. **A.** RT-qPCR assay. mRNA expression of CES1 and CTSC in peripheral blood from HCM patients and healthy people (control). *** $p < 0.001$ *vs.* Control group. **B.** mRNA expression of CES1 or CTSC was negatively correlated with Maxi LVWT. For abbreviations, see Figure 4.

with different expression and in the black module (Fig. 4D). Compared with the expression of mRNA in normal tissues, mRNA expression levels of CES1 and CTSC were downregulated in HCM tissues according to RNA sequencing data from GEO (GSE130036, $p < 0.001$, Fig. 4E). To further verify the lower expression of CES1 and CTSC in HCM, we analyzed another RNA expression profiles from GEO (GSE68316). Compared with the expression of mRNA in normal tissues, mRNA expression of CES1 and CTSC was also downregulated in HCM tissues ($p < 0.001$, Fig. 4E). The Pearson correlation coefficient was used to calculate the correlation between relative gene expression and Maxi LVWT in GSE130036 dataset. As shown in Figure 4F, the mRNA expression of CES1 and CTSC was negatively correlated with Maxi LVWT (cor = −0.48, $p < 0.001$; cor = −0.31, $p < 0.001$). In summary, the mRNA expression of CES1 and CTSC was downregulated in HCM and was negatively correlated with Maxi LVWT.

Table 3. Clinical features of samples from HCM patients

Clinical characteristics		
Age (year)	Media	31
	Mean	34.8
	Range	24–54
Sex (*n*)	Female	10
	Male	10
LAD (mm)	Media	41
	Mean	43
	Range	33–59
LVST (mm)	Media	19
	Mean	20.2
	Range	15–27
LVEDD (mm)	Media	45.7
	Mean	46
	Range	32–51
LVEF (%)	Media	69.5
	Mean	69.8
	Range	58–79
Maxi LVWT (mm)	Media	26
	Mean	24.2
	Range	16–38
Sample location	Peripheral blood	20

For abbreviations, see Table 1.

Clinical sample validation

In this study, peripheral blood samples were obtained from HCM patients ($n = 20$) or healthy people ($n = 20$) between November 2020 and May 2021 in the Kunming Yan'an Hospital (Kunming, China). We collected clinical information for all patients. The clinical features of the patients including sex, age, LAD, LVST, LVEDD, LVEF, Maxi LVWT and sample location, were collected from their medical records (Table 3). As shown in Figure 5A, the mRNA expression levels of CES1 and CTSC in the HCM groups were decreased to 27.29 ± 4.59% ($p < 0.001$) and 40.13 ± 1.09% ($p < 0.001$) of the normal groups respectively. As shown in Figure 5B, the HCM patients with low mRNA expression of CES1 or CTSC have higher values of Maxi LVWT (cor = 0.54, $p < 0.001$; cor = −0.34, $p < 0.001$). In summary, the study confirms the downregulated expression of CES1 and CTSC in HCM through clinical samples from HCM patients, and their expression was negatively correlated with Maxi LVWT.

Cell model validation

Angiotensin II (Ang II) has been clearly demonstrated to induce cardiomyocyte hypertrophy. We treated AC16 cells with Ang II (150 nM) for 24 h for HCM model construction. As shown in Figure 6A, protein/DNA ratio in the HCM groups was increased to 4.37 ± 0.51 ($p < 0.001$)-fold that of the control groups. The mRNA and protein expres-

sions levels of HCM markers (ANP, BNP and β-MHC) were significantly increased in the HCM groups, compared with the control groups (Fig. 6B,C). As shown in Figure 6D, the mRNA and protein expressions levels of CES1 and CTSC in the HCM model groups were downregulated compared with those in the control groups. In conclusion, we suggest that CES1 and CTSC are downregulated in the HCM cell model.

Overexpression of CES1 and CTSC can alleviate HCM progression

CES1 and CTSC genes were overexpressed in AC16 cells. After overexpressing CES1 and CTSC, the mRNA expression of CES1 and CTSC in AC16 cells was up-regulated, which was 6.19 ± 0.94 ($p < 0.001$)- or 7.21 ± 0.55 ($p < 0.001$)-fold of the control group (Fig. 7A). After overexpressing CES1 and CTSC, the protein expression of CES1 and CTSC in AC16 cells was also upregulated, which was 6.10 ± 0.66 ($p < 0.001$)- or 7.85 ± 0.94 ($p < 0.001$)-fold of the control group (Fig. 7B). We further examined the remission effect of overexpression of CES1 or CTSC on the HCM cell model. The protein/DNA ratio in Ang II-induced AC16 cells which were overexpressed of CES1 or CTSC was decreased to 59.98 ± 12.07% ($p < 0.001$) or 60.75 ± 13.23 % ($p < 0.001$) of the control (Fig. 7C). Under the same conditions, the mRNA and protein expression of HCM maker (ANG, BNG and β-MHC) were also decreased significantly, compared with that of the control. In summary, we suggest that overexpression of CES1 and CTSC can alleviate HCM progression.

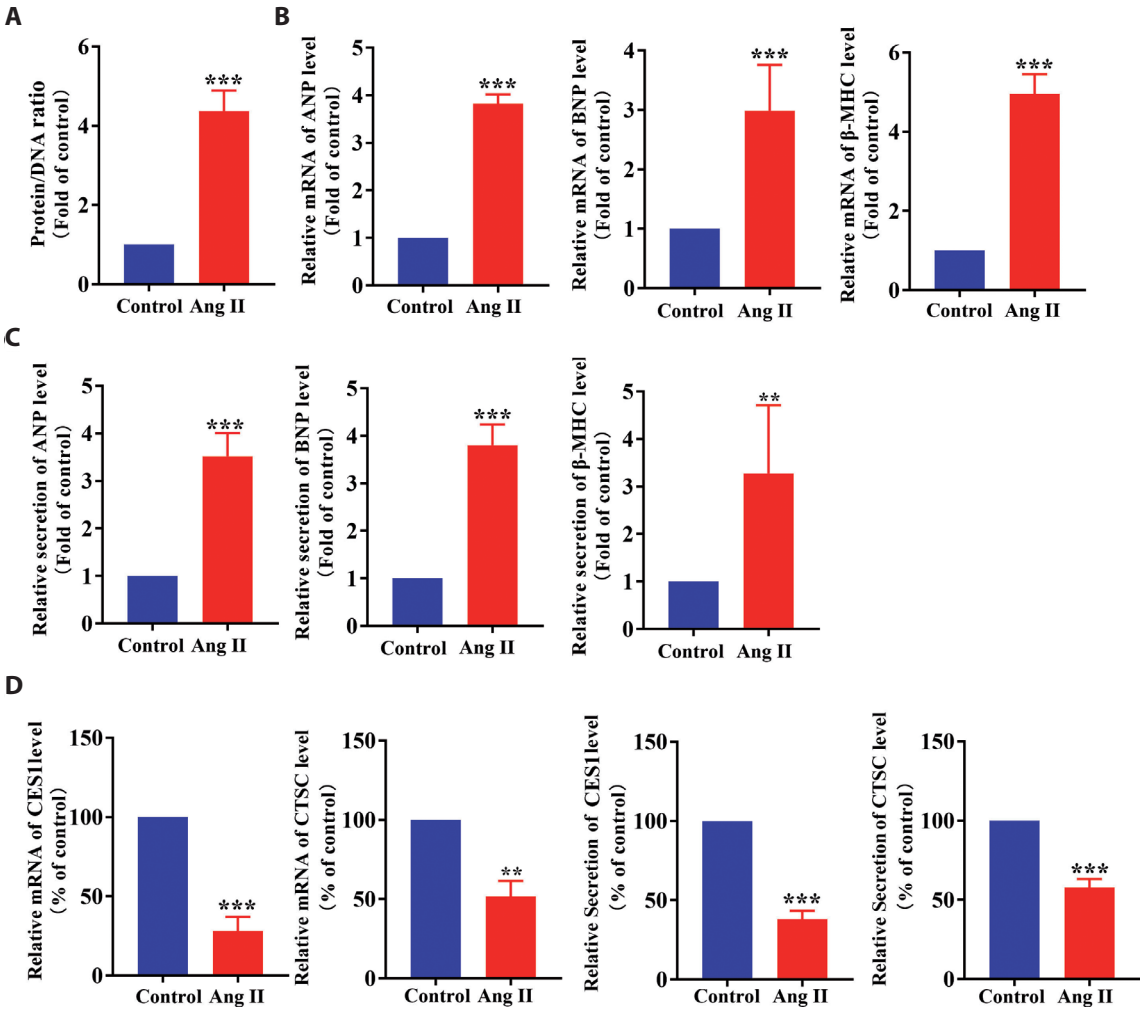

Figure 6. HCM cell model validation in AC16 cells treated with 150 nM Ang II. **A.** Protein/DNA ratio. **B.** The mRNA expression of ANP, BNP and β-MHC using RT-qPCR method. **C.** The protein expression of ANP, BNP and β-MHC using ELISA. **D.** The mRNA and protein expression of CES1 and CTSC. ** $p < 0.01$, *** $p < 0.001$ *vs.* Control group. ANP, atrial natriuretic peptide; BNP, brain natriuretic peptide; β-MHC, major histocompatibility complex beta; ELISA, Enzyme linked immunosorbent assay; Ang II, angiotensin II. For more abbreviations, see Figure 4.

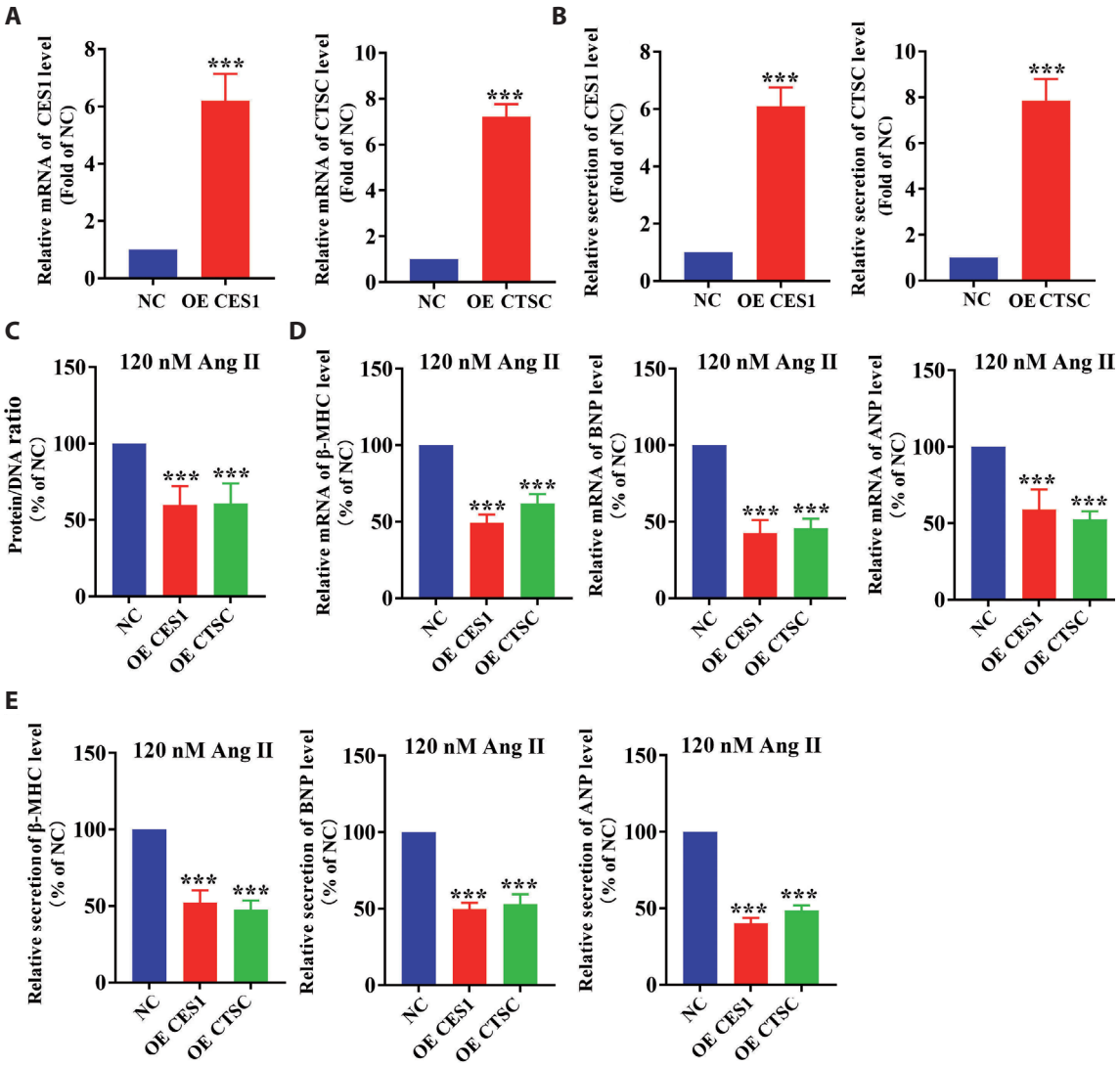

Figure 7. Overexpression of CES1 and CTSC can alleviate HCM progression. **A, B.** The mRNA or protein expression of CES1 or CTSC in AC16 cells overexpressing CES1 (OE CES1) or CTSC (OE CTSC) compared with the negative control (NC). **C.** Protein/DNA ratio in Ang II-induced AC16 cells which overexpressing CES1 or CTSC. **D, E.** The mRNA and protein expression of ANP, BNP and β-MHC in Ang II-induced AC16 cells which overexpressing CES1 or CTSC. *** $p < 0.001$ *vs.* NC group. For more abbreviations, see Figure 4 and 5.

Discussion

HCM is the most common hereditary cardiovascular disease with an incidence rate ranging from 0.16–0.29% in adults (Despond and Dawson 2018). At present, molecular genetics research shows that at least 40 genes and more than 1400 gene mutations have been confirmed to be associated with the clinical phenotype of HCM (Maron and Maron 2013). Gene detection plays an important role in HCM. It can not only be used to identify the cause of disease but also guide the family members of patients to carry out genetic screening. In recent years, research on biomarkers of HCM has been increasing. Chen et al. (2019) identified biomarkers correlated with hypertrophic cardiomyopathy with coexpression analysis. This study identified 2,351 differentially expressed genes based on the results of topological overlap measure-based clustering. This study further found that the TYROBP, CSF1R, and SYK genes were upregulated in HMC and closely related to the immune system of the body. Zheng et al. (2021) identified and verified biomarkers in patients with hypertrophic cardiomyopathy associated with immune cell infiltration characteristics. This study shows that neutrophils and B cells (primitive and memory B cells) are highly abundant in HCM samples through CIBERSORT analysis. SLITRK4 and CD163 were further identified to be closely related to neophils and B cells through WGCNA. In our

study, we found that CES1 and CTSC were downregulated in HCM and further found that they were negatively correlated with Maxi LVWT. Overexpression of CES1 and CTSC can alleviate HCM progression in a cell model.

CES1 encodes a member of the carboxylesterase large family. CES1 participates in fatty acyl and cholesterol ester metabolism, and plays a role in the blood-brain barrier system. More studies focus on the role of CES1 in liver diseases and drug metabolism (Shi et al. 2016; Yan et al. 2019; Her and Zhu 2020). For example, Na et al. (2020) reported that CES1 exerted an anti-proliferation effect on hepatocellular carcinoma through the PKD1/PKCμ signaling pathway. Chen et al. (2018) revealed the influence of gene structure polymorphism of CES1 and CES2 on drug metabolism, and evaluated the potential significance of their genetic variation on drug therapy. CTSC encodes a member of the peptidase C1 family and lysosomal cysteine proteinase. As an independent risk factor, CTSC has abnormal expression in a variety of cardiovascular diseases. For example, the expression of CTSC is up-regulated in patients with heart failure (Tang et al. 2008) and coronary heart disease (Fox et al. 2007). Some cardiovascular disease drugs, such as Wenxin Keli, can cause a decrease in CTSC in the patients with myocardial infarction (Zheng et al. 2016). However, CES1 and CTSC have not been studied in HCM. In our study, we found that CES1 and CTSC were down-regulated in HCM, and further found that they were negatively correlated with Maxi LVWT. Overexpression of CES1 and CTSC can alleviate HCM progression in cell model. The study suggests that CES1 and CTSC negatively regulate the development of HCM, and have potential as therapeutic and diagnostic targets for HCM.

Acknowledgements. We thank the Gene Expression Omnibus (GSE68316, GSE130036) project for providing data.

Funding. This work was supported by Joint Special Program of Applied Basic Research of Kunming Medical University – Young Doctor Program (Grant numbers: 202001AY070001-153).

Availability of data and materials. Public data are deposited at Gene Expression Omnibus (GEO, https://www.ncbi.nlm.nih.gov/geo/, GSE130036 and GPL20795, GSE68316 and GPL20113). Gene database of NCBI (National Center of Biotechnology Information, https://www.ncbi.nlm.nih.gov/gene/). The datasets generated during and analysed during the current study are available from the corresponding author on reasonable request.

Authors' contributions. All authors contributed to the study conception and design. Material preparation, data collection and analysis were performed by Ye Kuang, Jia Wang, Yulin Dong, Yun Cheng, Hongyan Li, Yong Ji, Hui Gao and Xianghong Cao. The first draft of the manuscript was written by Ye Kuang and all authors commented on previous versions of the manuscript. All authors read and approved the final manuscript.

Ethics approval and consent to participate. This study was approved by the Ethics Committee of the Kunming Yan'an hospital (2020; Kunming, China; approval No. 2019-058-01) and all patients signed informed consent.

Conflict of interest. The authors declare that they have no competing interests.

Reference

Canepa M, Pozios I, Vianello PF, Ameri P, Brunelli C, Ferrucci L, Abraham TP (2016): Distinguishing ventricular septal bulge versus hypertrophic cardiomyopathy in the elderly. Heart **102,** 1087-1094 https://doi.org/10.1136/heartjnl-2015-308764

Chen F, Zhang B, Parker RB, Laizure SC (2018): Clinical implications of genetic variation in carboxylesterase drug metabolism. Expert Opin. Drug Metab. Toxicol. **14,** 131-142 https://doi.org/10.1080/17425255.2018.1420164

Chen R, Ge T, Jiang W, Huo J, Chang Q, Geng J, Shan Q (2019): Identification of biomarkers correlated with hypertrophic cardiomyopathy with co-expression analysis. J. Cell Physiol. **12,** 21999-22008 https://doi.org/10.1002/jcp.28762

Despond EA, Dawson JF (2018): Classifying cardiac actin mutations associated with hypertrophic cardiomyopathy. Front. Physiol. **17,** 405 https://doi.org/10.3389/fphys.2018.00405

Efthimiadis GK, Pagourelias ED, Gossios T, Zegkos T (2014): Hypertrophic cardiomyopathy in 2013: Current speculations and future perspectives. World J. Cardiol. **6,** 26-37 https://doi.org/10.4330/wjc.v6.i2.26

Her L, Zhu HJ (2020): Carboxylesterase 1 and precision pharmacotherapy: Pharmacogenetics and nongenetic regulators. Drug Metab. Dispos. **48,** 230-244 https://doi.org/10.1124/dmd.119.089680

Josowitz R, Mulero-Navarro S, Rodriguez NA, Falce C, Cohen N, Ullian EM, Weiss LA, Rauen KA, Sobie EA, Gelb BD (2016): Autonomous and non-autonomous defects underlie hypertrophic cardiomyopathy in BRAF-mutant hiPSC-derived cardiomyocytes. Stem Cell Reports **7,** 355-369 https://doi.org/10.1016/j.stemcr.2016.07.018

Kamisago M, Sharma SD, DePalma SR, Solomon S, Sharma P, McDonough B, Smoot L, Mullen MP, Woolf PK, Wigle ED, et al. (2000): Mutations in sarcomere protein genes as a cause of dilated cardiomyopathy. N. Engl. J. Med. **343,** 1688-1696 https://doi.org/10.1056/NEJM200012073432304

Langfelder P, Horvath S (2008): WGCNA: an R package for weighted correlation network analysis. BMC Bioinformatics **29,** 559 https://doi.org/10.1186/1471-2105-9-559

Li J, Wu Z, Zheng D, Sun Y, Wang S, Yan Y (2019): Bioinformatics analysis of the regulatory lncRNA-miRNA-mRNA network and drug prediction in patients with hypertrophic cardiomyopathy. Mol. Med. Rep. **20,** 549-558 https://doi.org/10.3892/mmr.2019.10289

Liew AC, Vassiliou VS, Cooper R, Raphael CE (2017): Hypertrophic cardiomyopathy-past, present and future. J. Clin. Med. **6,** 118

https://doi.org/10.3390/jcm6120118
Liu X, Ma Y, Yin K, Li W, Chen W, Zhang Y, Zhu C, Li T, Han B, Liu X, et al (2019): Long non-coding and coding RNA profiling using strand-specific RNA-seq in human hypertrophic cardiomyopathy. Sci. Data **6,** 90
https://doi.org/10.1038/s41597-019-0094-6
Lu DY, Yalçin H, Yalçin F, Zhao M, Sivalokanathan S, Valenta I, Tahari A, Pomper MG, Abraham TP, Schindler TH, et al. (2018): Stress myocardial blood flow heterogeneity is a positron emission tomography biomarker of ventricular arrhythmias in patients with hypertrophic cardiomyopathy. Am. J. Cardiol. **121,** 1081-1089
https://doi.org/10.1016/j.amjcard.2018.01.022
Marian AJ, Braunwald E (2017): Hypertrophic cardiomyopathy: Genetics, pathogenesis, clinical manifestations, diagnosis, and therapy. Circ. Res. **121,** 749-770
https://doi.org/10.1161/CIRCRESAHA.117.311059
Maron BJ, Maron MS (2013): Hypertrophic cardiomyopathy. Lancet **381,** 242-255
https://doi.org/10.1016/S0140-6736(12)60397-3
Maron MS (2012): Clinical utility of cardiovascular magnetic resonance in hypertrophic cardiomyopathy. J. Cardiovasc. Magn. Reson. **14,** 13
https://doi.org/10.1186/1532-429X-14-13
Marques MdA, de Oliveira GAP (2016): Cardiac toponin and tropomyosin: Structural and cellular perspectives to unveil the hypertrophic cardiomyopathy phenotype. Front. Physiol. **7,** 429-429
https://doi.org/10.3389/fphys.2016.00429
Minarowska A, Minarowski Ł, Karwowska A, Milewska AJ, Gacko M (2012): Role of cathepsin A and cathepsin C in the regulation of glycosidase activity. Folia Histochem. Cytobiol. **50,** 20-24
https://doi.org/10.5603/FHC.2012.0003
Na K, Kim M, Kim CY, Lim JS, Cho JY, Shin H, Lee HJ, Kang BJ, Han DH, Kim H, et al. (2020): Potential regulatory role of human-carboxylesterase-1 glycosylation in liver cancer cell growth. J. Proteome Res. **19,** 4867-4883
https://doi.org/10.1021/acs.jproteome.0c00787
Pham CT, Armstrong RJ, Zimonjic DB, Popescu NC, Payan DG, Ley TJ (1997): Molecular cloning, chromosomal localization, and expression of murine dipeptidyl peptidase I. J. Biol. Chem. **272,** 10695-10703
https://doi.org/10.1074/jbc.272.16.10695
Rasmussen HB, Bjerre D, Linnet K, Jürgens G, Dalhoff K, Stefansson H, Hankemeier T, Kaddurah-Daouk R, Taboureau O, Brunak S, et al. (2015): Individualization of treatments with drugs metabolized by CES1: combining genetics and metabolomics. Pharmacogenomics **16,** 649-665
https://doi.org/10.2217/pgs.15.7
Schmittgen TD, Livak KJ (2008): Analyzing real-time PCR data by the comparative C(T) method. Nat. Protoc. **3,** 1101-1108
https://doi.org/10.1038/nprot.2008.73
Shen XB, Chen X, Zhang ZY, Wu FF, Liu XH (2021): Cathepsin C inhibitors as anti-inflammatory drug discovery: Challenges and opportunities. Eur. J. Med. Chem. **225,** 113818
https://doi.org/10.1016/j.ejmech.2021.113818
Shi J, Wang X, Nguyen J, Wu AH, Bleske BE, Zhu HJ (2016): Sacubitril is selectively activated by carboxylesterase 1 (CES1) in the liver and the activation is affected by CES1 genetic variation. Drug Metab. Dispos. **44,** 554-559
https://doi.org/10.1124/dmd.115.068536
Tang WH, Van Lente F, Shrestha K, Troughton RW, Francis GS, Tong W, Martin MG, Borowski AG, Jasper S, Starling RC, et al. (2008): Impact of myocardial function on cystatin C measurements in chronic systolic heart failure. J. Card. Fail. **14,** 394-399
https://doi.org/10.1016/j.cardfail.2008.01.006
Vakrou S, Fukunaga R, Foster DB, Sorensen L, Liu Y, Guan Y, Woldemichael K, Pineda-Reyes R, Liu T, Tardiff JC, et al. (2018): Allele-specific differences in transcriptome, miRNome, and mitochondrial function in two hypertrophic cardiomyopathy mouse models. JCI Insight **3,** e94493
https://doi.org/10.1172/jci.insight.94493
Wang Y, Wang Z, Yang Q, Zou Y, Zhang H, Yan C, Feng X, Chen Y, Zhang Y, Wang J, et al. (2013): Autosomal recessive transmission of MYBPC3 mutation results in malignant phenotype of hypertrophic cardiomyopathy. PLoS One **8,** e67087-e67087
https://doi.org/10.1371/journal.pone.0067087
Yan M, Zhang Z, Liu Z, Zhang C, Zhang J, Fan S, Yang Z (2019): Catalytic hydrolysis mechanism of cocaine by human carboxylesterase 1: An orthoester intermediate slows down the reaction. Molecules **24,** 4057
https://doi.org/10.3390/molecules24224057
Yang W, Li Y, He F, Wu H (2015): Microarray profiling of long non-coding RNA (lncRNA) associated with hypertrophic cardiomyopathy. BMC Cardiovasc. Disord. **15,** 62
https://doi.org/10.1186/s12872-015-0056-7
Zheng M, Liu Z, Liu N, Hou C, Pu J, Zhang S (2016): The effect of Wenxin Keli on the mRNA expression profile of rabbits with myocardial infarction. Evid. Based Complement. Alternat. Med. **2016,** 2352614
https://doi.org/10.1155/2016/2352614
Zheng X, Yang Y, Huang Fu C, Huang R (2021): Identification and verification of promising diagnostic biomarkers in patients with hypertrophic cardiomyopathy associate with immune cell infiltration characteristics. Life Sci. **285,** 119956
https://doi.org/10.1016/j.lfs.2021.119956

Received: September 14, 2022
Final version accepted: January 27, 2023

Doi: 10.4149/gpb_2023009

Supplementary Material

Weighted gene coexpression network analysis reveals negative regulation of hypertrophic cardiomyopathy by carboxylesterase 1 and cathepsin C

Ye Kuang, Jia Wang, Yulin Dong, Yun Cheng, Hongyan Li, Yong Ji, Hui Gao and Xianghong Cao

Department of Medical Laboratory, Yan'An Hospital of Kunming city, Kunming, China

Supplemengtary Table

Table S1. The differentially expressed mRNAs

	Gene symbol	logFC	*p* value	Change (HCM *vs.* Normal)
1	TNFRSF4	−1.509144244	0.007457568	down
2	DDAH1	−2.243817221	0.018146857	down
3	KCNC4	−3.143810001	2.41E−05	down
4	RGSL1	−2.605698954	0.040918383	down
5	PPFIA4	−2.139525032	6.34E−05	down
6	INHBB	−1.804126729	2.39E−05	down
7	LRP1B	−1.782713727	0.002487662	down
8	FAP	−1.702707842	0.003364683	down
9	TTN	−1.82768905	0.000666188	down
10	MSTN	−1.568571821	0.003213815	down
11	MAP2	−1.624741139	0.000132301	down
12	CXCR2	−2.203512521	0.018273688	down
13	ASB18	−1.758556701	2.63E−05	down
14	RASL11B	−1.946664429	4.75E−06	down
15	KIT	−1.708173342	0.002172176	down
16	IRX1	−1.614737342	7.53E−06	down
17	IL31RA	−2.459996777	0.008954971	down
18	SOX4	−1.514747702	4.05E−07	down
19	FAM65B	−1.877235872	9.97E−05	down
20	SFRP4	−2.320461607	7.78E−05	down
21	MYL7	−1.502206908	0.001085557	down
22	GCK	−1.66048736	0.006170661	down
23	XG	−1.70079755	0.029513782	down
24	ACE2	−2.272834282	5.47E−08	down
25	SYTL5	−2.459887356	0.000472229	down
26	SSX1	−1.739752294	0.032847474	down
27	SLITRK4	−2.477637876	2.71E−06	down
28	SLC6A8	−2.674902359	0.001633	down
29	CA3	−2.408090402	0.000181986	down
30	MAL2	−1.616136612	0.000945523	down
31	FAM219A	−1.783814606	0.027504135	down
32	RNF38	−1.907420946	0.040035378	down
33	PRUNE2	−1.526777569	0.01094676	down
34	BRINP1	−2.310433671	4.02E−08	down
35	BDNF	−2.313623719	8.87E−05	down
36	NXPH4	−2.112906229	0.00028885	down
37	HMGA2	−1.53235959	0.00374266	down
38	PHLDA1	−2.753633712	1.06E−05	down
39	CUX2	−1.788576613	0.002154652	down
40	POSTN	−1.826212321	0.001109656	down
41	PCDH17	−1.528405196	9.12E−08	down
42	FARP1	−2.042714572	3.02E−07	down
43	C14orf132	−1.712721524	2.46E−08	down
44	HBA2	−4.032102023	6.15E−08	down
45	PALM3	−1.811484241	0.001787322	down
46	CASP14	−2.043174441	0.012162319	down
47	PHLDB3	−1.713993846	0.049794005	down
48	APOC2	−1.560619628	0.016534965	down
49	KLK4	−1.737249368	0.037205597	down
50	KLK14	−1.538354549	0.046045192	down
51	IGLON5	−1.598636254	3.33E−08	down
52	NKG7	−1.820259429	0.008461125	down
53	LZIC	1.920997481	0.015243314	up
54	C1QC	1.998821431	5.77E−13	up
55	C1QB	2.586992169	4.15E−11	up
56	FCN3	2.149892709	0.000201749	up

(continued)

Table S1. (continued)

	Gene symbol	logFC	*p* value	Change (HCM *vs.* Normal)
57	THEMIS2	1.568165992	7.51E−06	up
58	RAB42	1.607622694	0.049525209	up
59	MACF1	3.561388892	0.032173809	up
60	CC2D1B	1.79308953	0.002576447	up
61	NFIA	2.20434	0.000850263	up
62	ST7L	1.582766022	0.002547595	up
63	AP4B1	1.854281356	0.002402533	up
64	CA14	1.664317079	0.000201468	up
65	MLLT11	1.633153755	0.007312485	up
66	SELENBP1	1.598391091	2.74E−10	up
67	PMVK	2.490098813	0.02037591	up
68	SDHC	1.529082747	0.000367363	up
69	FCGR2B	1.59023078	0.000151292	up
70	BRINP3	2.049317183	0.004655065	up
71	RGS1	1.542911641	0.039717394	up
72	DDX59	1.913767172	0.002032577	up
73	SPRTN	1.66851653	0.025697985	up
74	ALKAL2	2.412640886	0.000636655	up
75	COLEC11	1.554146151	0.019087819	up
76	NT5C1B	2.109591209	0.004944941	up
77	OSR1	2.145749804	0.001094702	up
78	ADCY3	2.281956623	0.005483336	up
79	C2orf71	1.883077591	8.21E−06	up
80	VIT	1.998249846	0.001226341	up
81	EFEMP1	1.768561831	0.001680034	up
82	TGFA	1.774004877	0.029087203	up
83	TGOLN2	1.572421238	0.023296451	up
84	FHL2	2.055557621	1.12E−07	up
85	TMEM37	1.854035627	0.004933689	up
86	TUBA3E	2.759455723	2.31E−05	up
87	CACNB4	3.480998279	0.007977392	up
88	ACVR1C	1.685911178	0.001497268	up
89	GRB14	1.96645115	0.010143958	up
90	KLHL23	2.358197109	0.000231203	up
91	STAT1	1.782989541	0.01062737	up
92	FTCDNL1	1.53133522	0.038337457	up
93	AOX1	1.770438239	0.002318316	up
94	SGPP2	1.958502409	0.003530965	up
95	SP140L	1.62721632	0.006920554	up
96	TIMP4	1.738175738	7.45E−10	up
97	CNTN3	1.740277011	0.004233936	up
98	NFKBIZ	2.01762772	0.001095854	up
99	LSAMP	2.500762076	1.85E−06	up
100	COL6A6	1.998034909	4.81E−09	up
101	TF	2.031094276	0.001229038	up
102	FAIM	1.552847686	0.00952691	up
103	TMEM41A	2.264484916	0.039987583	up
104	ADIPOQ	2.13792194	0.012664091	up
105	FGF12	3.034494714	1.14E−07	up
106	GP5	2.041683906	0.003791254	up
107	WDR53	1.65997543	0.000644216	up
108	S100P	1.744834205	0.038013939	up
109	SHISA3	2.576601704	2.64E−10	up
110	CORIN	3.598868257	5.66E−12	up
111	TXK	1.692664864	0.001685984	up
112	ADAMTS3	1.516606186	0.002436733	up
113	CDS1	2.033744866	6.15E−10	up
114	ADH1B	1.652888722	0.000345755	up
115	IL15	2.030309253	0.002397337	up
116	ANAPC10	1.695686764	0.003418286	up
117	NAF1	1.94558482	0.009901855	up
118	NKD2	2.623661324	7.68E−05	up
119	ADCY2	1.706198015	0.004032369	up
120	RANBP3L	1.927928469	0.003316964	up
121	C7	1.666548173	1.26E−07	up
122	NIM1K	2.80172539	0.012649104	up
123	CD180	1.840505133	0.007574462	up
124	SLC30A5	1.733289049	0.020437575	up
125	IQGAP2	1.728510085	3.09E−06	up
126	LHFPL2	1.632964002	5.10E−05	up
127	DMGDH	1.999836047	0.008898236	up
128	CAMK4	1.932285526	0.001405049	up
129	SAR1B	1.750686013	0.005729084	up
130	CD14	2.040946479	1.89E−07	up
131	FAM153B	1.598097564	0.022403811	up
132	ZNF346	1.666947583	0.00156819	up
133	F13A1	2.502613488	1.12E−07	up
134	NEDD9	1.600953613	7.50E−10	up
135	FKBP5	1.651748481	0.006294506	up
136	GNMT	1.801930191	4.65E−09	up
137	VEGFA	1.968154669	0.001926315	up
138	TDRD6	1.579633367	0.002366697	up
139	MLIP	1.720510239	8.15E−05	up
140	RP11−257K9.8	2.312900367	1.30E−09	up
141	KPNA5	2.996723459	1.88E−05	up
142	TCF21	1.510485459	5.94E−05	up
143	FAM221A	1.511315786	0.009591141	up
144	BMPER	1.755435087	0.000341604	up
145	POU6F2	2.543087579	0.000843483	up
146	MDH2	2.104021052	0.006213016	up
147	PON3	3.393881074	6.46E−06	up
148	NPTX2	1.911124832	8.51E−05	up

(continued)

Table S1. (continued)

	Gene symbol	logFC	*p* value	Change (HCM *vs.* Normal)
149	PDAP1	1.583442371	0.014017439	up
150	AZGP1	1.906936106	2.21E−07	up
151	PTPRZ1	2.219306676	0.00023649	up
152	VEGFD	2.121882672	2.43E−07	up
153	RPGR	3.735074181	2.87E−06	up
154	CHST7	1.868053457	6.76E−13	up
155	KANTR	1.515666417	0.006347609	up
156	VSIG4	2.302454791	1.12E−05	up
157	HMGB3	1.755251865	0.002781545	up
158	PEBP4	1.655540866	1.51E−06	up
159	CDCA2	2.519073494	5.86E−08	up
160	SCARA5	2.265541077	6.39E−10	up
161	SPIDR	1.652256891	6.66E−05	up
162	CEBPD	2.112271407	8.48E−06	up
163	TCF24	1.807257921	0.000630875	up
164	SBSPON	1.811612743	0.001923509	up
165	RALYL	1.772598331	0.004304461	up
166	PKHD1L1	2.985218087	2.53E−07	up
167	HAS2	2.296822548	0.000114177	up
168	FAM83A	1.961869963	3.56E−06	up
169	POU5F1B	1.592643591	0.010613058	up
170	SLA	2.272100193	2.13E−08	up
171	NAPRT	2.080969667	0.017512163	up
172	GPAA1	1.613685115	0.013797485	up
173	GPT	1.533855791	0.001316747	up
174	ACO1	1.797399669	0.043294801	up
175	RPP25L	3.293022215	0.007099071	up
176	DDX31	2.670057797	8.07E−05	up
177	OLFM1	1.550305378	0.005353815	up
178	LCN6	2.581689158	0.02046047	up
179	SAPCD2	1.694128215	0.02876042	up
180	TMEM9B	1.796654533	6.47E−06	up
181	LYVE1	2.199632511	4.25E−11	up
182	CYP2R1	2.019315017	0.000780079	up
183	IGSF22	1.526788316	0.010908193	up
184	IMMP1L	2.16335431	0.004441153	up
185	CREB3L1	1.519769323	0.003454164	up
186	MYBPC3	2.428420958	0.002303365	up
187	OR9Q1	1.919675604	0.004463943	up
188	MS4A4A	1.555098383	0.01215169	up
189	MS4A7	1.729159337	1.16E−06	up
190	BEST1	1.652610811	0.000436998	up
191	CARNS1	2.060374228	0.042796587	up
192	MRPL21	1.949425131	4.36E−07	up
193	CHRDL2	2.43843218	3.55E−08	up
194	MAP6	1.924738509	0.002169127	up
195	ALG8	1.592934618	0.018824832	up
196	CTSC	1.62855103	0.003905735	up
197	BIRC3	1.821084554	1.06E−12	up
198	MSANTD4	1.514197103	0.000832041	up
199	FDXACB1	1.639299301	0.021802808	up
200	IL10RA	1.991634802	0.000975183	up
201	C11orf63	2.442729257	0.000317315	up
202	SCN3B	1.944488124	0.002685841	up
203	NCAPD3	1.672054554	0.003776061	up
204	B3GAT1	1.711805052	0.006015252	up
205	ARMC3	2.574580434	0.000119998	up
206	LRRC20	1.501391195	0.000861861	up
207	SFRP5	1.665262727	8.15E−05	up
208	KCNIP2	2.070648092	7.97E−07	up
209	SFR1	3.067812914	0.00384853	up
210	CD4	1.751678937	1.05E−07	up
211	C1R	1.815164787	0.000163001	up
212	CD163	1.937660989	8.14E−05	up
213	GPRC5A	2.277902895	0.00024175	up
214	BCAT1	1.56364876	7.72E−10	up
215	MCRS1	2.181391715	0.004470354	up
216	FAIM2	2.46600935	0.003501215	up
217	GPD1	1.623005755	0.025886303	up
218	DGKA	2.261984645	0.026127419	up
219	IRAK3	1.935856108	2.80E−07	up
220	RP11−162P23.2	1.686852897	0.005498982	up
221	CCDC62	1.851130144	0.01114936	up
222	TMEM132C	2.332129055	1.73E−07	up
223	ADGRD1	1.782081095	6.39E−10	up
224	CRYL1	2.905044984	0.016126083	up
225	USP12	2.21220888	0.02893061	up
226	SERP2	3.998882038	0.000305861	up
227	TPT1	1.580721494	0.021989343	up
228	SLC7A8	1.506966384	7.22E−07	up
229	MYH6	2.277548873	0.001858147	up
230	TRIM9	1.556195197	0.010608509	up
231	FUT8	1.692055415	0.005362913	up
232	HSP90AA1	2.453289657	0.007768512	up
233	ZBTB42	1.739254354	0.001593243	up
234	IGDCC4	2.331440624	3.06E−05	up
235	IDH2	1.988246673	0.031538209	up
236	MCTP2	1.525192061	0.018697965	up
237	TSR3	1.966931477	0.048898435	up
238	MRPS34	1.666950663	0.019742696	up
239	C16orf71	1.842478263	0.020102405	up
240	TVP23A	2.325213956	0.003985911	up

(continued)

Table S1. (continued)

	Gene symbol	logFC	*p* value	Change (HCM *vs.* Normal)
241	CCP110	1.565591676	0.028532883	up
242	CHP2	1.594882043	0.007053514	up
243	RP11–812E19.9	1.599445744	0.00926183	up
244	CES1	2.374461207	0.000279698	up
245	MT2A	1.855772374	2.50E−07	up
246	ZNF19	1.743149697	0.004940775	up
247	HPR	1.741868842	0.002488724	up
248	FAM92B	2.319664581	0.00786461	up
249	RTN4RL1	2.346229419	0.004237726	up
250	SMTNL2	1.891544121	0.002743323	up
251	KCTD11	1.864102112	0.008607342	up
252	DNAH2	2.032999421	0.003994127	up
253	RASD1	2.647885697	2.11E−06	up
254	B9D1	1.543650416	0.029398072	up
255	TBC1D3I	1.612332748	0.00081638	up
256	LINC00672	1.550280304	0.003560426	up
257	PLEKHH3	2.318617741	0.003618811	up
258	TMEM100	1.597067606	0.001613601	up
259	EFCAB3	1.611825269	0.023372449	up
260	RGS9	1.850759762	0.009762204	up
261	SMIM5	1.731250925	0.000815678	up
262	ITGB4	1.55656057	0.019313859	up
263	CYTH1	2.20105027	0.001401675	up
264	SIGLEC1	1.723649547	6.83E−09	up
265	CHGB	1.904328837	1.02E−06	up
266	FLRT3	1.872774712	0.003210678	up
267	ADA	1.52893836	0.009129019	up
268	PLTP	1.796409105	5.37E−07	up
269	BMP7	2.950482921	0.00053707	up
270	CFD	2.382174874	3.82E−11	up
271	C19orf35	2.136909634	0.029155302	up
272	MPND	1.792465161	0.022668299	up
273	CLEC4M	1.549918606	0.019877889	up
274	INSL3	1.509679053	0.022715618	up
275	LRRC25	1.696026773	0.01498671	up
276	SPINT2	1.796241098	0.003152487	up
277	AP2S1	1.734114979	0.000248682	up
278	CARD8	1.554071447	0.004744989	up
279	ADM5	2.28891285	0.002768329	up
280	FPR3	1.548195549	9.33E−07	up
281	ZNF615	1.553091081	0.043248411	up
282	LILRB5	1.896495094	4.62E−12	up
283	PRODH	1.638654724	1.41E−05	up
284	TANGO2	2.639761015	0.000315509	up
285	MTFP1	2.019204204	0.007737196	up
286	MAFF	1.934616539	0.000451408	up
287	PARVB	1.68661129	0.027374098	up
288	FBLN1	1.733727479	6.21E−05	up
289	ADAMTS5	1.884777277	3.09E−08	up
290	DOPEY2	1.61590904	0.00015901	up
291	ABCG1	2.420007862	0.000660257	up